International Journal of Industrial Electronics, Control and Optimization © 2021 IECO
Vol. 4, No. 2, pp. 157-165, April (2021)

Multi-Channel sEMG-Based Joint Angles Estimation of Lower Limbs Utilizing Bidirectional Recurrent Neural Network

Rohollah Hasanzadeh Fereydooni [1,†], Hassan Siahkali[2], Heidar Ali Shayanfar [3], Amir Hooshang Mazinan [4]

[1,2,3,4] Department of Electrical Engineering, South Tehran Branch, Islamic Azad University, Tehran, Iran.

ABSTRACT

Nowadays, rehabilitative robots, which have received more attention in the field of rehabilitation, can help patients in the rehabilitation training and reduce therapist workload. This paper suggests the use of surface electromyography (sEMG) signals and a bidirectional neural network (BRNN) for the estimation of the joint angles of lower limbs. The input of BRNN is the preprocessed sEMG signals and its outputs are the estimated joint angles of knee, ankle, and hip. In order to prove the usefulness of the BRNN, four normal and healthy subjects and two patients suffering from spinal cord injury (SCI) took part in the experimental tests. The healthy subjects exercised two movement modes including leg extension and treadmill at various loads and speeds, while the SCI subjects conducted only the treadmill exercise. To record useful information, seven leg muscles were used and then the hip, knee, and ankle joint angles were acquired at the same time. The experimental results showed the satisfactory performance of the proposed method in the estimation of joint angles by employing surface electromyography signals for both groups. The proposed estimation method can be used to control the rehabilitation robot of SCI subjects based on sEMG signals.

Article Info

Keywords:
Bidirectional recurrent neural network, Joint angle estimation, Rehabilitation robots, sEMG signals

Article History:
Received 2020-04-11
Accepted 2020-11-11

I. INTRODUCTION

Nowadays, rehabilitative robots, which are increasingly drawing attention in the field of rehabilitation, can help patients in rehabilitation training and reduce therapist workload [1-3]. Presently, rehabilitation robots can be chiefly separated into two types: passive exercise and active exercise. The treadmill used in passive exercises is a traditional limited treatment. The active training has been shown to amend the reorganization of the cortical [4] and to perform better neuro-rehabilitation [5, 6].

During muscle activity, muscle cells generate a weakened electrical potential called sEMG. Surface electrodes sense these sEMG signals [7]. The diagnosis of neurological and neuromuscular problems [8, 9] and application in prosthetic devices such as lower limbs, smart wheelchairs, and prosthetic hands [10–12] can be mentioned as the main application of the sEMG signals. Conventionally, there are three ways to use the sEMG signals. For the first time, they were used as a switch signal to examine the human body in different movement modes [13-16]. By this technique, the amputated member was able to control the prosthetic hand or limb with the help of the remaining muscles [17, 18]. In [14], the sEMG property was extracted by the natural logarithm of root mean square root values, and four motions were classified by a fuzzy C-means clustering method. In [17], a linearized Gaussian hybrid network is proposed to detect EMG patterns for human-assisting manipulator control, and this method shows a high recognition rate for eight different hand movements. Also, the muscle force or torque is estimated by the sEMG signals. In this regard, a

[†]**Corresponding Author**: St_r_hassanzadeh@azad.ac.ir
Tel: +98-12345678,Fax: +98-12345679, Islamic Azad University
Department of Electrical Engineering, South Tehran Branch, Islamic Azad University, Tehran, Iran

number of muscle force models have been developed, such as the Hill muscle model [19] and the Hammerstein muscle model [20]. When a precise relationship is established, sEMG signals show the active patient torque representing the patient's motion intention, and the active training of the rehabilitation robot is frequently controlled by using the sEMG signals. In [21], using sEMG, two methods are proposed for active training of the exoskeleton robots: dynamic human body model and direct force control. The human body force on robots can be computed by the sEMG signals. For the third aspect, the accurate body position is computed by the sEMG signals [22-27]. After finding the relationship between the joint angles and the sEMG signal, an arbitrary feasible posture is tracked in the active training mode by a rehabilitation robot or synthetic device. In [25], a switching regime model is proposed to decode the sEMG activity of 11 muscles to a continuous representation of arm movement in the 3-D space. In [27], a method is proposed to provide volitional control of a knee prosthesis utilizing sEMG signals. The intention of the patient and the set-point angle of the knee joint are computed by sEMG signals. These people can control the artificial hand.

In many approaches, sEMG signals have been used to estimate the joint angles, such as EMG-driven neuromusculoskeletal (NMS) model [28], linear model [29,30], linear switching regime model [31], local approximation, and lazy learning method [32], support vector machine (SVM) method [33], and artificial neural networks (ANN) [34]. They have been suggested for special applications, but there are still difficulties such as accuracy of estimation, real-time and dynamic characteristics, robustness, and uniformity. In [28], dynamic elbow movement is predicted by the NMS model, which requires many physiological parameters. The linear model suggested in [29,30] cannot apparently be used to estimate the real-time joint angle because one of the model parameters (the maximum IEMG signal value) is varying hen hand movements are performed with different efforts. However, in this model, this parameter is set to a constant. In [32], the joint angles of the fingers are estimated by the local approximation and the lazy learning method. The performance of the method was satisfactory for prosthetic hand control, except that a large time delay was shown in the test results, particularly for the movement of the thumb. The effect of finger speed on the joint angle estimation was also disregarded. There are similar problems in [33].

Many papers have used artificial neural networks to estimate joint angles. However, the accuracy of the ANN in estimating the joint angles is not high. The main reasons are that the multilayer perceptron neural network (MLP) is the most common neural network structure in existing studies. The data scale and feature that are two-dimensional data are the input data of MLP, but joint angle estimation is a three-dimensional problem (time, feature, and data scale).

Though sEMG signals have very sophisticated properties, their definite characteristic is that when the human muscle contraction has no variations, their amplitude increases. The process of changing the amplitudes of the sEMG signals consists of useful information to estimate the angles. To increase the accuracy of estimating the joint angles, this paper suggests a bidirectional recurrent neural network to estimate the relation between the joint angles and sEMG signals and develop a nonlinear model. To confirm the effectiveness of the BRNN, four healthy subjects and two SCI patients participated in the experimental tests. Two motions including treadmill training and leg movement at various speeds and loads were performed by the healthy subjects, and the patients only performed treadmill training. The results show that the BRNN can satisfactorily estimate the joint angle using sEMG signals.

II. METHOD AND STRATEGY

A. Data acquisition

In clinics, SCI patients or stroke patients are improved by treadmill exercise and leg extension exercises. In order to acquire experimental data, four healthy subjects (three men, one woman, 28±3 years old, 171±8 cm height) took part in treadmill training and leg extension exercises. Two SCI patients (both males, 42±2 years old, 166±5 cm height) took part in the treadmill exercise only. Fig. 1 shows the acquisition of joint angle information and sEMG signals during the treadmill run by a healthy subject. To record information simultaneously, seven leg muscles including vastus rectus muscle (VR), vastus lateralis muscle (VL), semitendinosus muscle (SM), biceps muscle of thigh (BM), tibialis anterior muscle (TA), extensor pollicis longus (EP), and gastrocnemius muscle (GM) were used and the hip, knee, and ankle joint angles were acquired at the same time. The Biomonitor ME6000 was utilized for the acquisition of the sEMG signal from the muscles. Fig. 2 depicts the raw sEMG signals and joint angles for one healthy subject.



Fig. 1. A healthy participant on the treadmill with sEMG sensors on the leg muscles.

To use sEMG signals in estimating the joint angles, the raw data is to be preprocessed. For this purpose, three following steps are to be executed.

Step1: The 50Hz noise generated by the power supply is filtered and removed in the raw sEMG signals employing a fifth-ordered notch filter.

Step 2: The filtered sEMG signals are rectified.

Step 3: The following equation is used to compute the online moving average (OMA) of the sEMG signals:

$$E(t)=\sqrt{\frac{1}{N}\sum_{i=0}^{N}E(t-i)^2} \quad (1)$$

where N and E (t) denote the number of the segments (N = 200) and the voltage at its sampling point (the rate of the sampling is 2 kHz), respectively.

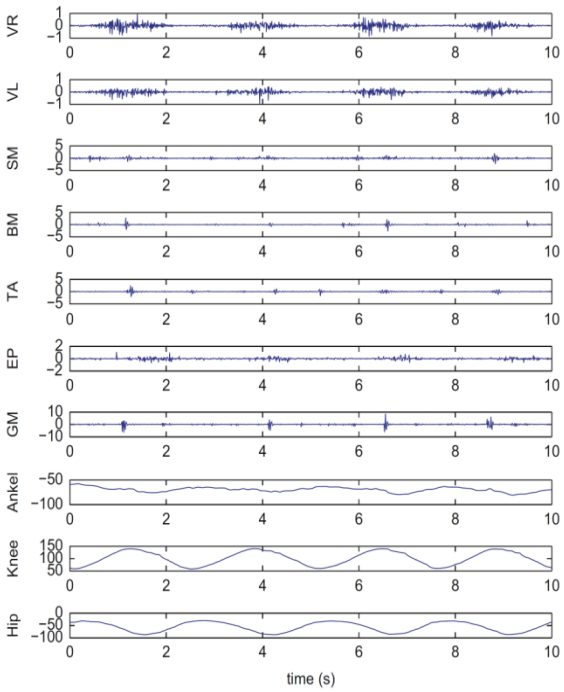


Fig. 2. Raw sEMG data acquired from seven muscles during treadmill exercise.

B. Estimation algorithm of using DRNN

As is seen in Fig. 3, the joint angles are estimated by the preprocessed sEMG signals along with the joint angle that are input signals for training the BRNN. The output of the BRNN is the estimated joint angles. In Fig. 3, the parameters a_j and θ are represented by:

$$\begin{cases}\theta=[\theta_1,...,\theta_i]\\ a_j=[a_{j,1},...,a_{j,i}]\end{cases} \quad (2)$$

where indexes i and j denote the number of acquired data and the number of sEMG channels, respectively.

III. BIDIRECTIONAL RECURRENT NEURAL NETWORK

A. The structure of BRNN

Unlike traditional neural networks, the connection between cells in the hidden layer of the RNN increases, meaning that input data of the hidden layer contains both the original data and the hidden cell state at the former time.

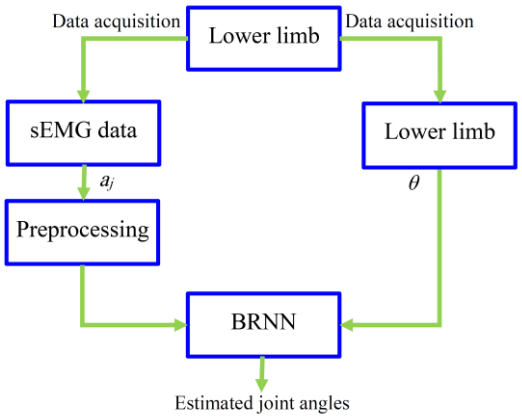


Fig. 3. Estimating the joints angles by the sEMG signal.

Considering an input sequence $x = (x_1, \ldots, x_T)$, an RNN calculates the hidden vector sequence $h = (h_1, \ldots, h_T)$ and output vector sequence $y = (y_1, \ldots, y_T)$ by iterating the following equations from $t = 1$ to T:

$$h_t = \mathrm{H}(W_{xh}x_t + W_{hh}h_{t-1} + b_h) \quad (3)$$

$$y_t = W_{hy}h_t + b_y \quad (4)$$

where W is connection weight matrices (for example, W_{xh} denotes the weight matrix from input to hidden), b is the bias vectors (for example, b_h denotes hidden bias vector), and H denotes the activation function.

H is normally the elementwise utility of the sigmoid function although the long short-term memory (LSTM) architecture, which utilizes purpose-built memory cells to store information, is better in finding and exploiting long-range data. A single LSTM memory cell is drawn in Fig. 4. In this paper, H is represented by the following functions:

$$i_t = \sigma(W_{xi}x_t + W_{hi}h_{t-1} + W_{ci}c_{t-1} + b_i) \quad (5)$$

$$f_t = \sigma(W_{xf}x_t + W_{hf}h_{t-1} + W_{cf}c_{t-1} + b_f) \quad (6)$$

$$c_t = f_t c_{t-1} + i_t \tanh(W_{xc}x_t + W_{hc}h_{t-1} + b_c) \quad (7)$$

$$o_t = \sigma(W_{xo}x_t + W_{ho}h_{t-1} + W_{co}c_t + b_o) \quad (8)$$

$$h_t = o_t \tanh(c_t) \quad (9)$$

where σ is the logistic sigmoid function and i, f, o, and c denote the input gate, forget gate, output gate, and cell activation vectors, respectively.

The connection weight matrices between the cell and gate vectors are diagonal, so the m-th element in each gate vector only accepts input from the m-th element of the cell vector.

One disadvantage of conventional RNN is that they can only utilize the previous data. To overcome this problem, bidirectional RNNs (BRNNs) [35] is used in this paper by processing the information in both directions with two separate hidden layers that are then fed forward to the same output layer.

It is clear from Fig. 5 that a BRNN calculates the forward

hidden sequence $\overrightarrow{h}$, the backward hidden sequence $\overleftarrow{h}$ and the output sequence y by iterating the backward layer from $t = T$ to 1, the forward layer from $t = 1$ to T, and then updating the output layer:

$$\overrightarrow{h}_t = \mathrm{H}\left(W_{x\overrightarrow{h}} x_t + W_{\overrightarrow{h}\overrightarrow{h}} \overrightarrow{h}_{t-1} + b_{\overrightarrow{h}} \right) \tag{10}$$

$$\overleftarrow{h}_t = \mathrm{H}\left(W_{x\overleftarrow{h}} x_t + W_{\overleftarrow{h}\overleftarrow{h}} \overleftarrow{h}_{t-1} + b_{\overleftarrow{h}} \right) \tag{11}$$

$$y_t = W_{\overrightarrow{h}y} \overrightarrow{h}_t + W_{\overleftarrow{h}y} \overleftarrow{h}_t + b_y \tag{12}$$

The bidirectional LSTM, which can access long-range data in both input directions, is constructed by combining BRNN with LSTM [16].

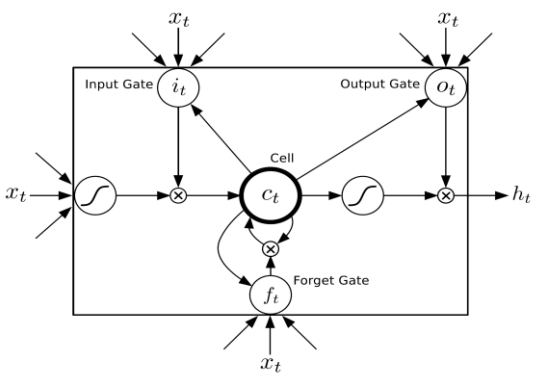


Fig. 4. Long short-term memory cell.

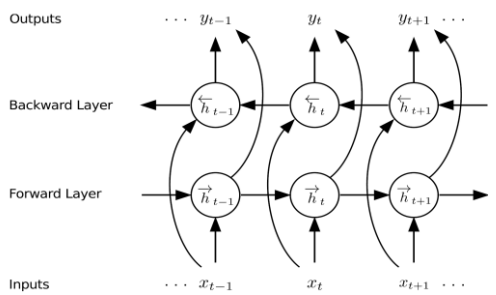


Fig. 5. Bidirectional RNN.

B. *Steps of estimation*

There are four steps in estimating the joint angles using the proposed BRNN:

- Step 1: Build up the BRNN;
- Step 2: Prepare sEMG data;
- Step 3: Train the BRNN. The inputs and outputs of the BRNN are the sEMG signal and the joint angles, respectively. The mean square error selected as the cost function is minimized by the algorithm of backpropagation through time (BPTT) [36].
- Step 4: Verify BRNN. A number of data acquired in step 2 are used to verify the trained BRNN model.

IV. Experimental Results

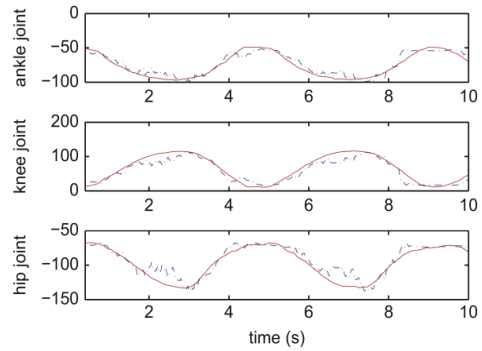
A. *Results*

Despite the simultaneous recording of sEMG signals from seven muscles, it should be noted that all channels do not contain useful information. It is clear from Fig. 2 that only sEMG of vastus rectus muscle, vastus lateralis muscle, and extensor pollicis longus contain very good dynamic data. Experimentally, the remaining of muscle signals was not utilized. Hence, the number of inputs as well as the complexity of the BRNN can be decreased. For every healthy subject, two BRNNs were created for the treadmill and leg extension exercises. Each input vector of the BRNN has a size of 40 including sEMG signal and the pervious samples. All BRNNs are trained by using back error propagation algorithm with a learning rate of 0.01 and random initial weights in the range of [-0.5; 0.5].

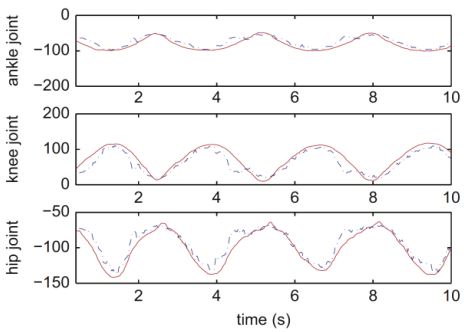
Figs. 6 and 7 depict the estimations of hip, knee, and ankle joint angles of a healthy subject in different conditions. From these figures, the suggested method works better in estimating the hip, knee, and ankle joint angles for fast speed regardless of the load during leg extension exercise. In fact, all four healthy subjects felt it was easier to do the exercise in a quick way that could give them a natural feeling. On the contrary, if they did this relatively slowly, four healthy subjects would feel uncomfortable since they could not control the speed and the slow speed would make them feel no rhythm. Regular and stable signals were generated when the subject had a sense of rhythm.

Similar results are presented in Fig. 7. The accuracy of the joint angles estimation is better in fast speed than in slow speed. From Fig. 7 (b), it is clear that the use of sEMG signals makes a more accurate estimate of the hip joint, knee joint, and ankle joint angles, and the mean angle error was less than 4.8 degrees for all four healthy persons during the treadmill exercise in fast speed with small load. As it is clear in Fig. 7(a) and (c), the estimation of the ankle joint angle is not as satisfactory as the estimation of the joint angles of the knee and hip principally because ankle control is not very natural while exercising at a slow pace. The estimation of the joint angles in fatigue mode (persons felt muscle pain and they did the exercise very hard) is illustrated in Fig. 7(d). Only the knee joint and hip joint angle are shown in this figure because the estimation error of the ankle joint is very large and we deliberately eliminated it. The mean estimation errors of the knee joint angle and the hip joint angle are also big (about 12.781 degrees). This is mainly because when subjects exercise in very fatigue conditions, the leg muscles contract very unstable with trembling of the limbs and in this case, the relationship between the sEMG signals and the angles of the joints becomes much more complicated. For two SCI patients, a BRNN was created for every subject. In Fig. 8, the estimation of the joint angles of the three joints for both subjects is shown, and the results are nearly as

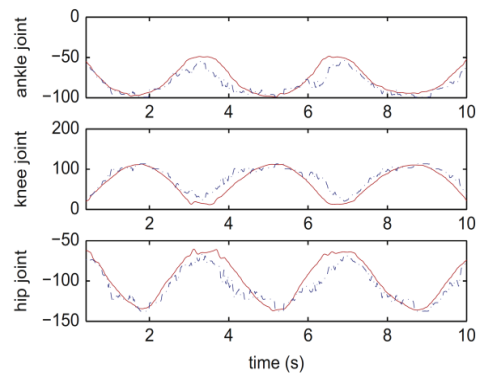
satisfactory as that of the health people. As is seen in Fig. 8, the first subject's ankle joint angle fluctuated to a greater extent during the treadmill exercise because this subject was unable to fully control his legs due to SCI. The second subject performed better in the estimation of the joint angles with a mean error of 2.631 degrees. This should be due to minimal damage to the spinal cord, so the sEMG signals were more stable in this subject than in the other subject.



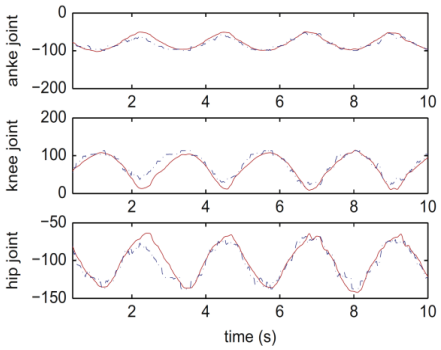
a



b



c



d

Fig. 6. Results obtained from leg extension exercise for a healthy subject. Solid lines (actual angles); dashed lines (estimated angles). (a) Leg extension with slow speed and small load, (b) leg extension with fast peed and small load, (c) leg extension with slow speed and big load, (d) leg extension with fast peed and big load.

Based on the comparison of Figs. 7 and 8, it is obvious that the estimation error of the healthy subjects is bigger than that of the SCI patients. The mean error for the healthy subjects is approximately 8.71 degrees during the leg extension exercise and approximately 5.91 degrees during the treadmill exercise regardless of the results under the fatigue mode, whereas the mean error for the SCI subjects is approximately 4.41 degrees during the treadmill exercise. This is associated with the fact that the movement range of healthy people is bigger than that of the SCI people.

In order to assess the performance of the angle estimation, Pearson's correlation coefficient (PCC) and root mean square error (RMSE) were employed. The PCC and RMSE are computed by:

$$PCC = \frac{\sum \theta_{act,n}\theta_{est,n} - \frac{\sum \theta_{act,n}\sum \theta_{est,n}}{N}}{\sqrt{\left(\sum \theta_{act,n}^2 - \frac{\left(\sum \theta_{act,n}\right)^2}{N}\right)\left(\sum \theta_{est,n}^2 - \frac{\left(\sum \theta_{est,n}\right)^2}{N}\right)}} \quad (13)$$

$$RMSE = \sqrt{\frac{1}{N}\sum_{n=1}^{N}\left(\theta_{act,n} - \theta_{est,n}\right)^2} \quad (14)$$

where $\theta_{act,n}$ and $\theta_{est,n}$ are the measured and estimated angles and N denotes the number of the samples.

Table I provides the values of PCC for four healthy subjects and two SCI patients. The values of RMSE for all cases are given in Table II. All these tests are performed for the leg extension test and hip angle.

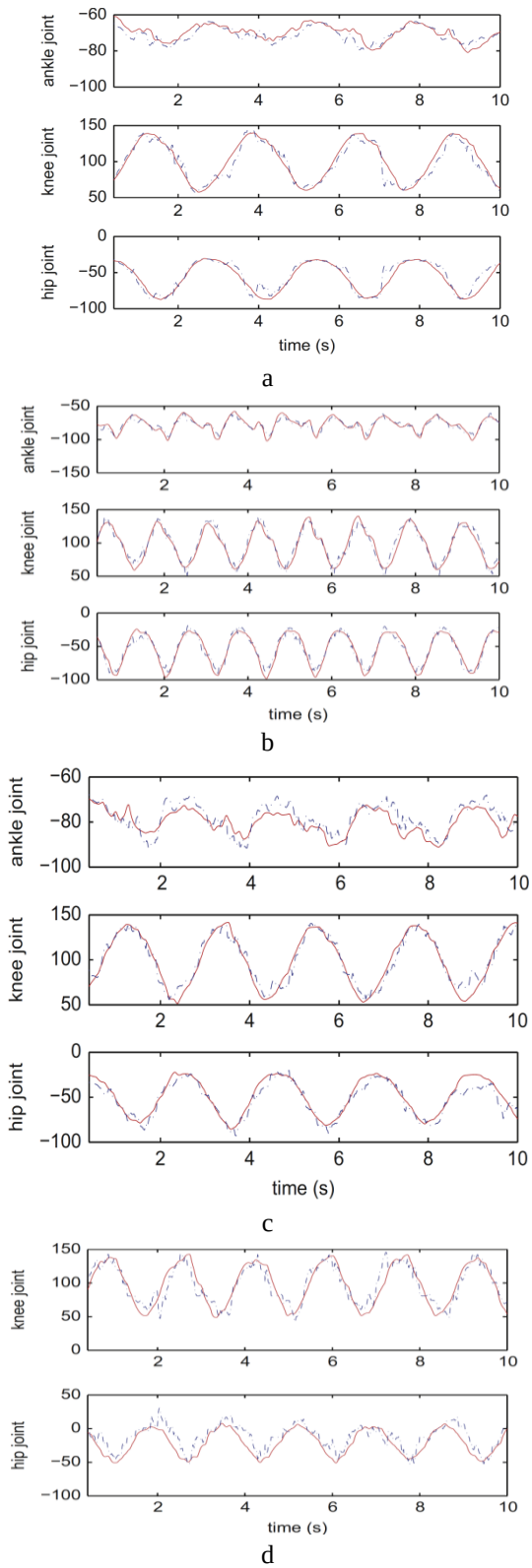


Fig. 7. Results obtained from treadmill exercise for a healthy subject. Solid lines (actual angles); dashed lines (estimated angles). (a) Treadmill exercise with slow speed and small load, (b) treadmill exercise with fast peed and small load, (c) Treadmill exercise with slow speed and big load, (d) treadmill exercise with fatigue.

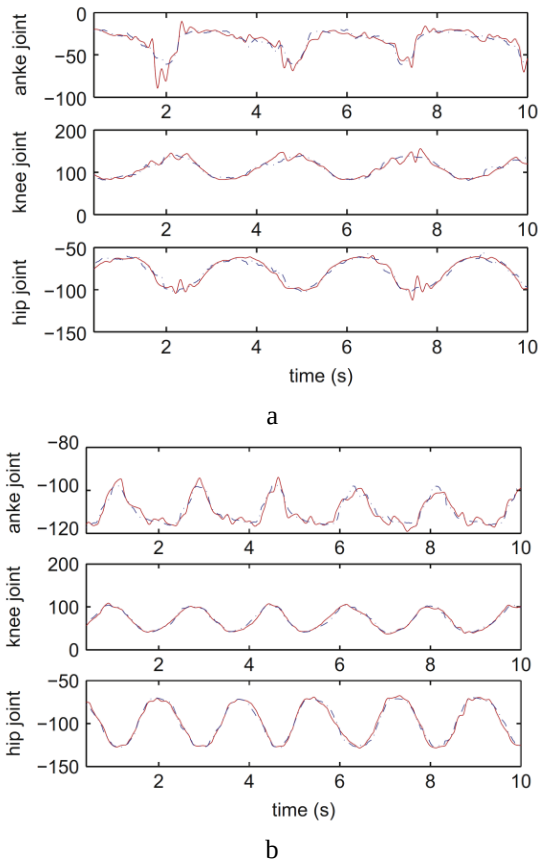


Fig. 8. Results obtained for SCI subjects. Solid lines (actual angles); dashed lines (estimated angles). (a) The first patient, (b) the second patient.

TABLE I
THE VALUES OF PCC FOR HEALTHY SUBJECTS AND SCI PATIENTS.

	Healthy subject				SCI patient	
	S_1	S_2	S_2	S_4	P_1	P_2
Mean	0.968	0.975	0.979	0.985	0.972	0.975
SD	0.013	0.008	0.006	0.003	0.009	0.007
Median	0.970	0.978	0.981	0.986	0.974	0.978
Maximum	0.983	0.984	0.987	0.990	0.981	0.988
Minimum	0.940	0.960	0.969	0.980	0.946	0.963

TABLE II
THE VALUES OF RMSE FOR HEALTHY SUBJECTS AND SCI PATIENTS.

	Healthy subject				SCI patient	
	S_1	S_2	S_2	S_4	P_1	P_2
Mean	9.761	8.882	8.831	8.804	9.865	8.954
SD	1.663	2.138	1.453	1.377	1.754	1.733
Median	10.031	9.329	9.104	8.951	9.430	9.324
Maximum	12.554	10.490	9.802	9.800	10.199	10.086
Minimum	8.780	7.663	7.232	6.895	7.545	7.433

B. Discussion

Based on the results, it can be confirmed that the joint angles of human legs can be satisfactorily estimated by sEMG signals in two modes of treadmill training and leg extension. The estimation of joint angles employing the

BRNN leads to good performance in both spinal patients and healthy people. Compared to traditional angle estimation methods, this approach improves angle estimation precision, characteristics of dynamic and real-time, and robustness. For all healthy people, the average error for leg extension and treadmill exercise are less than 9 degrees and 6 degrees, respectively, while these errors for SCI patients are 5 degrees due to a smaller range of motion. The sampling rate of the sEMG signals is 2 kHz, implying a time delay of 0.5ms. The performance of the proposed method is acceptable despite this time delay. Different speeds and loads are considered in the suggested approach and the results show a robust performance. The smoothness of estimating the joint angles is improved by the suggested method. According to the results, it can be concluded that these signals can be implemented for active training in a better way on the rehabilitation robot for spinal cord and stroke patients.

V. Conclusion

In this study, the sEMG signals are utilized to find a new human–robot interface. A neural network is employed to find the relationship between joint angles and sEMG signals, and practicability of this approach is confirmed by different experiments in healthy people as well as in SCI patients. To develop the nonlinear model, a bidirectional recurrent neural network is proposed. The BRNN is trained by the joint angles and sEMG signals and then used to estimate the joint angles that is usable in controlling rehabilitation robots. There is also a detailed discussion about estimating joint angles under different conditions such as various speeds and loads and in fatigue conditions and the proposed approach shows satisfactory robustness to various situations. Compared with the conventional techniques of estimating joint angles using the sEMG signals, this method improves many features, including the accuracy of the estimation, real-time specification, smoothness, dynamic specification, and robustness.

Appendix

Consider the following candidate Lyapunov function:

$$V(t)=\frac{1}{2}e^{T}(t)e(t) \tag{A.1}$$

where

$$e(t)=y^{*}(t)-y(t) \tag{A.2}$$

and y^{*} is the desired output. The convergence of the system can be `` if:

$$\Delta V(t+1)=V(t+1)-V(t)\le 0 \tag{A.3}$$

By combining (A.1) and (A.3), we have:

$$\Delta V(t+1)=\frac{1}{2}\left[2e(t)+\Delta e(t+1)\right]^{T}\Delta e(t) \tag{A.4}$$

where $\Delta e(t+1)=e(t+1)-e(t)$.

By combining (3), (4) and (A.2), and the use of Taylor series expansion, we can write the linear form of $e(t)$ as follows:

$$e(t+1)=e(t)+\frac{\partial e(t)}{\partial P(t)}\left[\Delta P(t)\right]^{T}+R' \tag{A.5}$$

where $P=[W, b]$, R' is the ignored higher-order terms.

Theorem 1. *Let η be the learning rate of the BRNN. The convergence is ensured if the learning rate satisfies:*

$$0<\eta<\frac{2}{\left(\frac{\partial e(t)}{\partial P(t)}\right)\left(\frac{\partial e(t)}{\partial P(t)}\right)^{T}} \tag{A.6}$$

Therefore, the convergence is ensured and $e(t)\to 0$ as $t\to\infty$.

Proof. (A.4) can be rewritten and simplified as follows:

$$\Delta V(t+1)=\frac{1}{2}e^{T}(t)e(t)\left\|\frac{\partial e(t)}{\partial P(t)}\right\|^{2}\left\{\eta\left\|\frac{\partial e(t)}{\partial P(t)}\right\|^{2}-2\right\} \tag{A.7}$$

If (A.6) is satisfied by the learning rate η, then:

$$\eta\left\|\frac{\partial e(t)}{\partial P(t)}\right\|^{2}-2<0 \tag{A.8}$$

In (A.7), η is positive, $e^{T}(t)e(t)$ and $\left\|\frac{\partial e(t)}{\partial P(t)}\right\|^{2}$ are zero or positive. Hence, by the use of (A.7) and (A.8), we conclude that:

$$\Delta V(t+1)\le 0 \tag{A.9}$$

Thus, the convergence of the BRNN can be ensured by using Lyapunov stability theorem.

References

[1] Yang, T., Gao, X., Gao, R., Dai, F., & Peng, J. (2019). A Novel Activity Recognition System for Alternative Control Strategies of a Lower Limb Rehabilitation Robot. *Applied Sciences*, 9(19), 3986.

[2] Qin, F., Zhao, H., Zhen, S., Sun, H., & Zhang, Y. (2020). Lyapunov Based Robust Control for Tracking Control of Lower Limb Rehabilitation Robot with Uncertainty. *International Journal of Control, Automation and Systems*, 18(1), 76-84.

[3] Wang, A., Hu, N., Yu, J., Liao, W., Zhang, J., Wu, X., & Pei, C. (2019, August). Research on robot control system of lower limb rehabilitation robot based on human gait comfort. *In 2019 International Conference on Advanced Mechatronic Systems (ICAMechS)* (pp. 34-39). IEEE.

[4] M. Lotze, C. Braun, N. Birbaumer, S. Anders, L.G. Cohen, Motor learning elcited by voluntary, *Brain 126* (2003) 866–872.

[5] L.L. Cai, A.J. Fong, C.K. Otoshi, Y. Liang, J.W. Burdick, R.R. Roy, V.R. Edgerton, Implications of assist-as-needed

robotic step training after a complete spinal cord injury on intrinsic strategies of motor learning, *Neuroscience* 26 (4) (2006) 10564–10568.
[6] G. Rosati, P. Gallina, S. Masiero, Design implementation and clinical tests of a wire-based robot for neurorehabilitation, *IEEE Trans. Neural Syst. Rehabil*. Eng. 15 (4) (2007) 560–569.
[7] G. Kamen, D. Gabriel, Essentials of Electromyography, Human Kinetics Publishers, USA, 2009.
[8] M.J. Zwarts, G. Drost, D.F. Stegeman, Recent progress in the diagnostic use of surface EMG for neurological diseases, *J. Electromyogr. Kinesiol*. 10 (5) (2000) 287–291.
[9] S.L. Pullman, D.S. Goodin, A.I. Marquinez, S. Tabbal, M. Rubin, Clinical utility of surface EMG: *report of the therapeutics and technology assessment subcommittee of the American Academy of Neurology*, *Neurology* 55 (2) (2000) 171–177.
[10] C. Cipriani, F. Zaccone, S. micera, M.C. Carrozza, On the shared control of an EMG-controlled prosthetic hand: analysis of user-prosthesis interaction, *IEEE Trans. Robot*. 24 (1) (2008) 170–184.
[11] T.A. Kuiken, G. Li, B.A. Lock, R.D. Lipschutz, L.A. Miller, K.A. Stubblefifield, K.B. Englehart, Targeted muscle reinnervation for real-time myoelectric control of multifunction artifificial arms, *J. Am. Med. Assoc*. 301 (6) (2009) 619–628.
[12] Y. Oonishi, O. Sehoon, Y. Hori, A new control method for power-assisted wheelchair based on the surface myoelectric signal, *IEEE Trans. Ind. Electron*. 57 (9) (2010) 3191–3196.
[13] F. Zhang, P.F. Li, Z.G. hou, X.L. Xie, Y.X. Chen, Q.L. Li, M. Tan, An adaptive RBF neural network control strategy for lower limb rehabilitation robot, *ICIRA 2010* (2010) 417–427.
[14] K. Momen, S. Krishnan, T. Chau, Real-time classifification of forearm electromyographic signals corresponding to user-selected intensional movements for multifunction prosthesis control, *IEEE Trans. Neural Syst. Rehabil. Eng.* 15 (4) (2007) 535–542.
[15] Y.H. Liu, H.P. Huang, C.H. Weng, Recognition of electromyographic signals using cascaded kernel learning machine, *IEEE Trans. Mechatron*. 12 (3) (2007) 253–264.
[16] D. Tkach, H. Huang, T. Kuiken, Study of stability of time-domain features for electromyographic pattern recognition, *J. Neuroeng. Rehabil*. 5 (2010) 7–21.
[17] O. Fukuda, T. Tsuji, M. kaneko, A. Otsuka, A human-assisting manipulator teleoperated by EMG signals and arm motions, *IEEE Trans. Robot. Autom*. 19 (2) (2003) 210–222.
[18] S. Yu, M.H. Fisher, A. Wolczowski, G.D. Bell, D.J. Burn, R.X. Gao, Towards an EMG-controled prosthetic using a 3-D electromagnetic positioning system, *IEEE Trans. Instrum. Meas.* 56 (1) (2007) 178–186.
[19] N.A. Shrirao, N.P. Reddy, D.R. Kosuri, Neural network committees for finger joint angle estimation from surface EMG signals, *Biomed. Eng. OnLine* 8 (2) (2009) 1–11.
[20] A.V. Hill, The heat of shortening and the dynamic constants of muscle, *Proc. R. Soc. Lond. B 126* (1938) 136–195.
[21] C. Fleischer, A. Wege, K. Kondak, G. Hommel, Application of EMG signals for controlling exoskeleton robots, Biomed. Tech. 51 (5) (2006) 314–319.
[22] C.A.M. Doorenbosch, J. Harlaar, Accuracy of a practicable EMG to force model for knee muscles, *Neurosci. Lett.* 368 (1) (2004) 78–81.
[23] G.L. David, F.B. Thor, An EMG-driven musculoskeletal model to estimate muscle forces and knee joint moments in vivo, *J. Biomech.* 36 (2003) 765–776.
[24] Q. Shao, N.B. Daniel, K. Manal, S.B. Thomas, An EMG-driven model to estimate muscle forces and joint moments in stroke patients, *Comput. Biol. Med*. 39 (12) (2009) 1083–1088.
[25] P.K. Artemiadis, K.J. Kyriakopoulos, A switching regime model for the EMG-based control of a robot arm, *IEEE Trans. Syst. Man Cybern. Part B: Cybern.* 41 (1) (2011) 53–63.
[26] P.K. Artemiadis, K.J. Kyriakopoulos, EMG-based position and force estimates in coupled human-robot systems: towards EMG-controlled exoskeletons, *Springer Tracts Adv. Robot.* 54 (2009) 241–250.
[27] K.H. Ha, H.A. Varol, M. Goldfarb, Volitional control of a prosthetic knee using surface electromyography, *IEEE Trans. Biomed. Eng*. 58 (1) (2011) 144–151.
[28] K.K. Koo Terry, F.T. Mak Arthur, Feasibility of using EMG driven neuromusculoskeletal model for prediction of dynamic movement of the elbow, *J. Electromyogr. Kinesiol.* 15 (2005) 12–26.
[29] Y. Masahiro, M. Masahiko, T. Kazuyo, Real time hand motion estimation using EMG signals with support vector machines, *in: SICE-ICASE International Joint Conference*, 2006, pp. 593–598.
[30] Y. Masahiro, M. Masahiko, T. Kazuyo, Hand pose estimation using EMG signals, *in: IEEE International Conference on EMBS*, 2007, pp. 4830–4833.
[31] N.P. Reddy, V. Gupta, Toward direct biocontrol using surface EMG signals: control of fifinger and wrist joint models, *Med. Eng. Phys.* 29 (2007) 398–403.
[32] A. Christian, C. Cipriani, M. Controzzi, M.C. Carrozza, G. Lundborg, B. Rose´n, F. Sebelius, Using EMG for real-time prediction of joint angles to control a prosthetic hand equipped with a sensory feedback system, *J. Med. Biol. Eng.* 30 (6) (2010) 399–406.
[33] J. Shi, Y. Zheng, Z. Yan, SVM for estimation of wrist angle from sonomyography and sEMG signals, *in: IEEE International Conference on EMBS*, 2007, pp. 4806–4809.
[34] K.J. Hunt, M. Munih, N.deN. Donaldson, F.M.D. Barr, Investigation of the hammerstein hypothesis in the modeling of electrically stimulated muscle, *IEEE Trans. Biomed. Eng.* 45 (8) (1998) 998–1009.
[35] M. Schuster and K. K. Paliwal, "Bidirectional Recurrent Neural Networks," *IEEE Transactions on Signal Processing*, vol. 45, pp. 2673–2681, 1997.
[36] Farahani, Mohsen. "A multi-objective power system stabilizer." *IEEE Transactions on Power Systems* 28.3 (2012): 2700-2707.



Rohollah Hasanzadeh Fereydooni received his B.Sc. degree in Robotic Engineering at the Shahrood University of Technology, Iran in 2011 and his M.Sc. degree in Mechatronic Engineering at South Tehran Branch, Islamic Azad University, Tehran, Iran in 2014. He is now a Ph.D. candidate in Control Engineering at South Tehran Branch, Islamic Azad University. His research interests include rehabilitation robots, robotics, and intelligent systems.
E-mail: st_r_hassanzadeh@azad.ac.ir (Corresponding author).



Hassan Siahkali was born in Tehran, Iran. He received his B.S. degree in Electronics Engineering at Tabriz University, Tabriz, Iran, in 1993, and his M.S. and Ph.D. degrees in Electrical Engineering at the Amir Kabir University of Technology and Sharif University of Technology, Tehran, Iran, in 1996 and 2010, respectively. From 1999 to 2006, he was with Niroo Research Institute, Tehran, Iran. From 2006 to 2012, he worked as the manager of Energy and System Studies Center at the MONENCO Consulting Engineer Company, Tehran, Iran. In 2006, he joined Islamic Azad University –South Tehran Branch as an assistant professor in Engineering Faculty. His current research interests include power system operation and planning, electricity markets, and power system quality.



Heidar Ali Shayanfar was born in Zabol, Iran, on March 11, 1951. He received his B.S. and M.S.E. degrees in Electrical Engineering in 1973 and 1979 and his Ph.D. degree in Electrical Engineering at Michigan State University, U.S.A., in 1981. Currently, he is a full professor at the Electrical Engineering Department of Iran University of Science & Technology (lUST), Tehran, Iran. His research interests are the application of artificial intelligence to power system control design, dynamic load modeling, power system observability studies, voltage collapse, applications of facts devices in power systems, and restructured power systems.



Amir Hooshang Mazinan received his Ph.D. degree in Control Engineering in 2009. He is currently an associate professor and the director of Control Engineering Department at IAU South Tehran Branch starting from 2009. His research interests include intelligent systems, model-based predictive control, over-actuated space systems modeling and control, time frequency representation, filter banks, wavelet theory, and image-video processing.

IECO

This page intentionally left blank.